



## Rapid communication

## Predicting burst sizes in amorphous alloys during plastic flows

J.W. Qiao<sup>a,b,\*</sup>, Z. Wang<sup>a,b</sup>, Z.M. Jiao<sup>c</sup>, H.J. Yang<sup>a,b,\*\*</sup>, S.G. Ma<sup>c</sup>, Z.H. Wang<sup>c</sup>, B.S. Xu<sup>a,b,d</sup><sup>a</sup> Laboratory of Applied Physics and Mechanics of Advanced Materials, College of Materials Science and Engineering, Taiyuan University of Technology, Taiyuan 030024, China<sup>b</sup> Key Laboratory of Interface Science and Engineering in Advanced Materials, Ministry of Education, Taiyuan University of Technology, Taiyuan 030024, China<sup>c</sup> Institute of Applied Mechanics and Biomedical Engineering, Taiyuan University of Technology, Taiyuan 030024, China<sup>d</sup> Research Center of Advanced Materials Science and Technology, Taiyuan University of Technology, Taiyuan 030024, China

## ARTICLE INFO

## Article history:

Received 10 April 2014

Accepted 1 May 2014

Available online 14 May 2014

## Keywords:

Bulk amorphous alloys

Failure

Plasticity

Shear bands

## ABSTRACT

Burst sizes in different amorphous alloys are predicted by  $\Delta\sigma = \sqrt{(2l_v E \rho c_p (0.8T_g - T_r))} / 0.9aD \sin \theta$ . When the diameter of tested samples is decreased, the burst size is greatly increased. And the critical diameter, corresponding to shear failure, could be predicted. The present prediction could be as a criterion to guarantee steady serrations free of failure.

Crown Copyright © 2014 Published by Elsevier B.V. All rights reserved.

## 1. Introduction

Many crystalline alloys exhibit irregular plastic flows observed as a jerky-flow (stress serration) or strain-staircase behavior after yielding upon loading. For instance, there is a repetitive localized yielding during the plastic deformation of 5XXX Al–Mg alloys, which is the so-called Portevin–Le Châtelier (PLC) effect due to the dynamic strain ageing (DSA) during which solute atoms diffuse around dislocations and retard dislocation motion, leading to negative strain rate sensitivity and thus to material instabilities during plastic flows [1,2]. Analogously, serrated flow is a characteristic feature during the plastic deformation of amorphous alloys. Kimura et al. [3] found similar serrated flows in bulk metallic glasses upon uniaxial compressive loading. Schuh and Nieh [4] have found that Pd- and Zr-based bulk metallic glasses (BMGs) exhibit serrated flows during nanoindentation, manifested as a stepped load–displacement curve punctuated by discrete bursts of plasticity. Besides, Yang et al. [5] revealed the jerky flows in micropillars of Mg-, Fe-, Cu-, and Zr-based amorphous alloys. In the absence of dislocations, the plastic deformation of amorphous alloys is governed by the formation and propagation of shear

bands. After yielding, amorphous alloys exhibit jerky flows on the stress–strain curves related to shear banding, which accommodates the plastic deformation.

Usually, the burst sizes of the serrated flows with a statistical magnitude decrease with the increasing strain rates [6]. Sun et al. [7] investigated the dynamic behavior of serrated flows in amorphous alloys and discovered that the plastic flows could evolve into a self-organized state, characterized by the power-law distribution of shear avalanches. Recently, the origin of serrated flows has been revealed; serrated flows in fact arise from an intrinsic dynamic instability of the shear band sliding, which was determined by a critical stiffness parameter in stick–slip dynamics [8]. The dynamics of serrated flows in amorphous alloys has been widely studied [5–12]. However, predicting burst sizes of serrated flows responsible for the dynamics phenomena is still poorly understood. In this study, we will estimate the burst sizes by relating the shear banding behavior with the energy conversion during serrated flows in amorphous alloys.

## 2. Results and discussion

The typical serration phenomena on the stress–strain curve of amorphous alloys after yielding is schematically shown in Fig. 1. After yielding, serrated flows dominate the uniaxial compressive stress–strain curves, including following two stages: stress ascending and stress drops, both of which have different physical processes but very similar amplitudes. In the former stage, elastic loading on the whole samples prevails, accompanied by the accumulation of strain energy within the samples. In the following

\* Corresponding author at: Laboratory of Applied Physics and Mechanics of Advanced Materials, College of Materials Science and Engineering, Taiyuan University of Technology, Taiyuan 030024, China. Tel.: +86 351 6018051.

\*\* Corresponding author at: Laboratory of Applied Physics and Mechanics of Advanced Materials, College of Materials Science and Engineering, Taiyuan University of Technology, Taiyuan 030024, China.

E-mail addresses: [qiaojunwei@gmail.com](mailto:qiaojunwei@gmail.com) (J.W. Qiao), [pineyang@126.com](mailto:pineyang@126.com) (H.J. Yang).

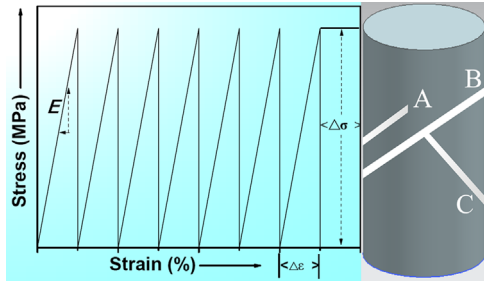


Fig. 1. The typical serration phenomena in the stress–strain curve of amorphous alloys after yielding schematically shown.

stage, shear avalanche occurs, dissipating the storage energy. Generally, the burst event happens in the latter stages, manifested by shear banding, as schematically shown in Fig. 1. It can be seen that profuse shear bands are distributed on the lateral surface of the samples, closely related with the plastic serrated flows.

Although the serrated flows are very common in amorphous alloys, the amplitudes of stress drops in different metallic glass formers differ largely [13]. How to predict the burst sizes is still a big challenge. Obviously, the amplitudes of stress ascending and stress drops are similar, and thus, we can estimate the amplitude of the stress ascending instead. The storage elastic energy in unit volume,  $w$ , could be calculated by the following equation:

$$w = \frac{1}{2} \Delta\sigma \Delta\varepsilon \quad (1)$$

where  $\Delta\sigma$  and  $\Delta\varepsilon$  are the amplitude of stress ascending and corresponding strain during one serration, as schematically shown in Fig. 1. As a result, the total storage elastic energy during one serration is estimated to be

$$W = wV_{total} \quad (2)$$

where  $V_{total}$  is the volume of the tested sample. During energy dissipation, it is usually assumed that the amorphous alloys experience adiabatic heating [14,15]. Here, it is considered that a thin layer or hot region, form instantly, with a homogeneous temperature. In other words, about 90% of mechanical work converts into heat at the moment of stress bursts. At the final fracture, the temperature can reach thousands of Kelvin [14], and melted features can be found on the whole fracture surface [16]. It should be noted that once the viscous layer is generated, the friction within it would not withstand the shearing, followed by shearing failure. However, the burst sizes during stress serrations are distinguishingly lower than the yielding stress, and then the mechanical work accumulated in one serration is much lower than the dissipated energy at the final fracture. Therefore, the dissipation of strain energy during serrations would not lead to the catastrophic failure. Instead, steady serrations dominate.

It is assumed that the temperature within shearing layers is less than  $0.8T_g$  ( $T_g$  is the glass-transition temperature) during serrations, since a significant softening usually takes place for amorphous alloys at this temperature [17]. If the temperature reaches or exceeds  $0.8T_g$ , the viscous fluid could not prohibit dynamic fracture. Thus, the heat generated,  $H$ , by shearing during one serration is calculated to be

$$H = \frac{\pi D^2 l_v}{4 \sin \theta} \rho c_p (0.8T_g - T_r) \quad (3)$$

where  $D$  is the diameter,  $l_v$  is the thickness of the shearing layer,  $\rho$  is the density,  $c_p$  is the heat capacity, and  $T_r$  is the room temperature with a value of about 298 K. According to the energy balance,  $0.9W = H$ . The residual mechanical work will convert into

electric and/or light energy [18]. Thus, the following is obtained:

$$0.9 \times \frac{1}{2} \Delta\sigma \Delta\varepsilon V_{total} = \frac{\pi D^2 l_v}{4 \sin \theta} \rho c_p (0.8T_g - T_r) \quad (4)$$

Usually,  $V_{total} = (\pi D^2 / 4) aD$ , where  $a$  is the aspect ratio of the tested samples ( $a = l/D$ ). And  $\Delta\sigma = E \Delta\varepsilon$ , where  $E$  is the Young modulus of amorphous alloys. By substituting  $a$  and  $E$  into Eq. (4), the following is obtained:

$$\Delta\sigma = \sqrt{\frac{2l_v E \rho c_p (0.8T_g - T_r)}{0.9aD \sin \theta}} \quad (5)$$

After collecting lots of data from different glass-forming systems, the data (experimental and predicted values) is plotted in Fig. 2. The parameters in Eq. (5) are summarized in Table 1 [19–35]. These glass-forming systems include Zr- [9,10,19–24,26–28,30,31,35], Pd- [25], Cu- [29], Au- [32], and Mg-based [33,34] amorphous alloys. It is noted that  $l_v$  in Eq. (5) is taken to be 100 nm [15,20], analogous to the thickness of the hot region. The fracture angle is taken to be  $45^\circ$  with respect to the loading direction. In the present estimation, it is simply assumed that the whole shearing plane is formed, as schematically indicated by a “B” shear layer in Fig. 1. Actually, not all burst events result in integrated shearing planes, and many “half” shear planes prevail instead, as schematically indicated by “A” and “C” shear layers in Fig. 1. Thus, the predication may overestimate the burst sizes.

It can be seen that the experimental values are very close to the predicted values, calculated by Eq. (5). For example, Wright et al. [24] obtained a maximum burst size of 40 MPa in Zr-based BMGs under the strain rate of  $10^{-4}/s$ . In comparison, according to Eq. (5), a burst size of 55 MPa is predicted. In addition, Dubach et al. [35] obtained a maximum burst size of about 1 GPa in a Zr-based nanopillar with a diameter of  $3 \mu m$ , and the predicted value is 1.55 GPa. The experimental and predicted results are comparable.

It should be noted that the experimental value is taken from the maximum burst sizes during serrations. The lower the strain rate is, the larger is the burst size. In the present study, the collected data is generally under the strain rate range of  $10^{-4}$ – $10^{-3}/s$ . If the strain rate is decreased further, the experimental burst size is definitely increased, and as a result, the experimental values are closer to the predicted ones. Based on the above analysis, Eq. (5) is a powerful tool to predict the burst sizes of amorphous alloys under quasi-static loading.

Fig. 3(a) shows the experimental and predicted burst size with the diameter for a typical glass-forming system – the  $Zr_{41.25}Ti_{13.75}Ni_{10}Cu_{12.5}Be_{22.5}$  amorphous alloy. It can be seen that when the size of tested samples is decreased, the burst size is greatly increased in spite of experimental or predicted values. Here, the diameter and length of  $Zr_{41.25}Ti_{13.75}Ni_{10}Cu_{12.5}Be_{22.5}$  amorphous alloys are marked in Fig. 3(a), and the calculated prediction curve is based on the aspect ratio of 2.5. The current

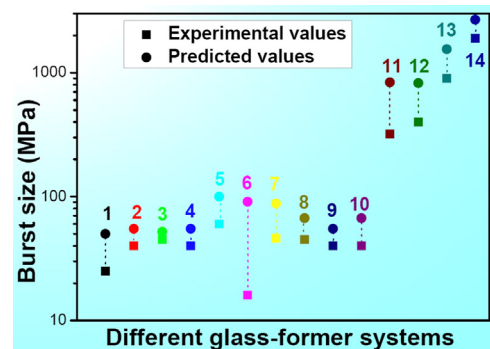


Fig. 2. The burst sizes from the experimental and predicted results in different glass-forming systems.

Download English Version:

<https://daneshyari.com/en/article/1575167>

Download Persian Version:

<https://daneshyari.com/article/1575167>

[Daneshyari.com](https://daneshyari.com)